DOI 10.1007/s10778-022-01117-6
International Applied Mechanics, Vol. 57, No. 6, November, 2021

NONLINEAR VIBRATIONS AND DISSIPATIVE HEATING OF LAMINATED SHELLS OF PIEZOELECTRIC VISCOELASTIC MATERIALS WITH SHEAR STRAINS*

V. I. Kozlov[1], L. P. Zinchuk[1], and T. V. Karnaukhova[2]

A combined numerical-and-analytical technique for studying the forced geometrically nonlinear vibrations of laminated shells of revolution made of piezoelectric viscoelastic materials under electrical and mechanical loadings with allowance for transverse shear strains and temperature of dissipative heating is proposed. The technique is based on the finite-element method in the variational statement and the harmonic linearization method. The results of numerical modeling of a hinged three-layer cylindrical panel consisting of similar outer piezoelectric layers and inner passive viscoelastic layer are presented. The behavior of the deflection in the neighborhood of the first resonance for cylindrical panels of different thickness is studied. The temperature field of vibroheating of the viscoelectroelastic cylindrical panel under electrical loading is analyzed numerically.

Keywords: forced vibrations, geometric nonlinearity, piezoelectric layer, shell of revolution, finite-element method, temperature of dissipative heating

Introduction. Multilayer plates and shells made of piezoelectric viscoelastic materials are widely used in various fields of modern engineering. These structures should meet strict requirements for dimensions and possible mechanical displacements and strains under acting loads and operating temperatures. Forced harmonic vibrations are main modes of operation of these structures. Harmonic electromechanical loading with frequency close to resonance may result in intensive vibrations and intensive heating depending on the loading level and heat transfer conditions. The increase in the temperature known as dissipative heating [4, 15] is attributed to hysteresis losses. It should be noted that the physical and mechanical characteristics of a number of piezoelectric materials make it possible to design thin-walled members with allowance for their operation with considerable displacements. To simulate the electromechanical vibrations of such members, various hypotheses are employed. In the case of very thin members made of viscoelastic materials, the use of classical Kirchhoff–Love hypotheses may cause considerable errors in calculating vibration damping and distribution of dissipative heating temperature. For this reason, it is important to develop methods of geometrically nonlinear analysis of the dynamic behavior of piezoelectric viscoelastic plates and shells at resonant frequencies with allowance for the dissipative heating and transverse shear strains.

The main approaches to the analysis of the nonlinear dynamics of elastic plates and shells are detailed in [6, 9–12, 21–23].

---

[1]Tymoshenko Institute of Mechanics, National Academy of Sciences of Ukraine, 3 Nesterova St., Kyiv, 03057, Ukraine; e-mail: term@inmech.kiev.ua. [2]National Technical University of Ukraine “Igor Sikorsky Kyiv Polytechnic Institute,” 37 Peremogy Av., Kyiv, 03056, Ukraine; e-mail: karn@inmech.kiev.ua. Translated from Prikladnaya Mekhanika, Vol. 57, No. 6, pp. 61–80, November–December 2021. Original article submitted February 28, 2020.

* This study was sponsored by the budgetary program Support of Priority Areas of Research (KPKVK 6541230).

In this connection, the papers [14, 24, 25, 27] should be mentioned among a few publications on the geometrically nonlinear vibrations of inhomogeneous plates and shells with piezoelectric layers. Electromechanical models of the behavior of laminated thin-walled members made of inelastic piezoelectric materials and the effect of dissipative heating, geometrical and physical nonlinearities on their dynamic behavior are addressed in [15–17]. The finite-element method, whose features are considered in [1, 13, 25], is the most universal numerical method of solving nonlinear problems for inhomogeneous plates and shells.

The present paper is devoted to the development of a combined numerical and analytical technique of studying the forced nonlinear vibrations of laminated viscoelastic piezoelectric shells of revolution and dissipative heating temperature under mechanical and electrical loadings at resonant frequencies with allowance for transverse shear strains. We will consider laminated shells using the Timoshenko-type hypothesis and nonlinear Karman theory supplemented with hypotheses for the electrical quantities. It is assumed that the components of electric-field strength and the normal component of the electric-flux density are nonzero, while the temperature field is distributed quadratically within each layer and the physical and mechanical parameters are independent of the temperature and electrical fields.

We will use the variational finite-element method. To approximate the displacements and geometry of the shell within a finite element, cubical polynomials will be used, while the deflection will be approximated by Hermite bicubic polynomials. The derived matrix equation will be solved using the classic method of expansion of unknowns into series of harmonics that are determined by solving generalized eigenvalue and eigenfunction problem in the electroelastic case. This makes it possible to reduce the matrix equation of motion to a second-order differential equation with nonlinear quadratic and cubic terms, which can be solved with the harmonic linearization method [2].

To validate the technique developed, we will consider the problem of the forced vibrations of a hinged viscoelectroelastic cylindrical sandwich panel of symmetric form under either mechanical or electrical loading. For this purpose, we will derive a nonlinear differential equation with respect to time by expanding the solution into a double trigonometric series. We will analyze the behavior of the deflection of cylindrical panels of various thicknesses at the principal resonance and compare the results obtained using the Kirchhoff–Love hypotheses and technique [20] with those found numerically using the refined Timoshenko-type theory.

Also, using the approach [7, 18] and the finite-element method to solve the nonstationary thermal-conduction problem, we will analyze the temperature field for the above-mentioned hinged viscoelectroelastic cylindrical panel under an electrical load.

1. Variational Problem Statement. As noted in [1, 3], the Timoshenko theory is one of the theories widely used to analyze the stress–strain state of inhomogeneous plates and shells with the finite-element method (FEM). This is due to the fact that the functionals appearing in variational formulations of the problems include only the first derivatives of the displacements. In developing the FEM, the variant of the so-called five-modal theory is employed in the nonlinear shell theory. In this theory, the displacement field is defined by five independent functions, which are the deflection w, two tangential displacements of the mid-surface u_0 and v_0, and two functions u_1 and v_1 defining the independent rotation of the normal:

$$u(s,\theta,z)=u_0(s,\theta)+zu_1(s,\theta),$$

$$v(s,\theta,z)=v_0(s,\theta)+zv_1(s,\theta),$$

$$w(s,\theta,z)=w(s,\theta). \tag{1.1}$$

Consider a sandwich shell of revolution with thickness $H=h_1+h_2+h_3$ consisting of transversely isotropic viscoelastic piezoelectric layers with thickness polarization. The shell is described in a curvilinear orthogonal coordinate system (s,θ,z). Let the mid-surface of the inner layer be the datum. The meridian of this surface is described by the equation $r=r(x)$. The surfaces $z=a_0, a_1, a_2, a_3$ are covered with either solid or discrete electrodes to which potentials V_0, V_1, V_2, V_3 are applied.

The equations of state relating stresses and strains are derived using the refined theory [4] that takes into account transverse shear strains and is supplemented with hypotheses for electrical qunatities. In this case, it is assumed that the components of electric-field strength and the normal component of electric-flux density $(D_z\neq 0, D_s=0, D_\theta=0)$ are nonzero.

Using the above hypotheses for the electromechanical quantities, Timoshenko's shear theory, and the classical equations of state for piezoelectric media [4, 8], the equations of state for the kth layer of the shell are as follows:

$$\sigma_{ss}^{(k)} = B_{11}^{(k)} \varepsilon_{ss} + B_{12}^{(k)} \varepsilon_{\theta\theta} - \gamma_{11}^{(k)} E_z^{(k)},$$

$$\sigma_{\theta\theta}^{(k)} = B_{12}^{(k)} \varepsilon_{ss} + B_{11}^{(k)} \varepsilon_{\theta\theta} - \gamma_{11}^{(k)} E_z^{(k)},$$

$$\sigma_{s\theta}^{(k)} = 2G_{12}^{(k)} \varepsilon_{s\theta}, \quad \sigma_{sz}^{(k)} = 2G_{13}^{(k)} \varepsilon_{sz}, \quad \sigma_{\theta z}^{(k)} = 2G_{23}^{(k)} \varepsilon_{\theta z},$$

$$D_z^{(k)} = \gamma_{33}^{(k)} E_z^{(k)} + \gamma_{11}^{(k)} (\varepsilon_{ss} + \varepsilon_{\theta\theta}), \tag{1.2}$$

where

$$B_{11}^{(k)} = c_{11}^{E(k)} - (c_{13}^{E(k)})^2 / c_{33}^{E(k)}, \quad B_{12}^{(k)} = c_{12}^{E(k)} - (c_{13}^{E(k)})^2 / c_{33}^{E(k)},$$

$$\gamma_{11}^{(k)} = e_{13}^{(k)} - c_{13}^{E(k)} e_{33}^{(k)} / c_{33}^{E(k)}, \quad \gamma_{33}^{(k)} = \mu_{33}^{S(k)} + (e_{33}^{(k)})^2 / c_{33}^{E(k)},$$

$$2G_{12}^{(k)} = c_{11}^{E(k)} - c_{12}^{E(k)}, \quad G_{13}^{(k)} = G_{23}^{(k)} = c_{44}^{E(k)} + (e_{15}^{(k)})^2 / \mu_{11}^{S(k)}, \tag{1.3}$$

where $c_{ij}^{E(k)}$ and $e_{ij}^{(k)}$ are the viscoelastic and piezoelectric moduli; $\mu_{ij}^{S(k)}$ are the dielectric permittivities of the piezoelectric material of the kth layer.

In what follows, we will consider shells for which z / R_1 and z / R_2 can be neglected compared with unity (R_1 and R_2 are the radii of principal curvatures of the mid-surface). Using the Karman nonlinear theory of thin-walled elements, expressions (1.1), and Cauchy's relations, we obtain the components of the strain tensor [15]:

$$\varepsilon_{ss} = \varepsilon_{ss}^0 + \kappa_{ss} z, \quad \varepsilon_{\theta\theta} = \varepsilon_{\theta\theta}^0 + \kappa_{\theta\theta} z, \quad \varepsilon_{s\theta} = \varepsilon_{s\theta}^0 + \kappa_{s\theta} z,$$

$$\varepsilon_{ss}^0 = \frac{\partial u_0}{\partial s} + \frac{w}{R_1} + \frac{1}{2}\left(\frac{\partial w}{\partial s}\right)^2, \quad \varepsilon_{\theta\theta}^0 = \frac{1}{r}\frac{\partial v_0}{\partial \theta} + \frac{\cos\varphi}{r} u_0 + \frac{w}{R_2} + \frac{1}{2}\left(\frac{\partial w}{r\partial \theta}\right)^2,$$

$$\varepsilon_{s\theta}^0 = \frac{1}{2}\left(\frac{\partial v_0}{\partial s} + \frac{1}{r}\frac{\partial u_0}{\partial \theta} - \frac{\cos\varphi}{r} v_0 + \frac{\partial w}{\partial s}\frac{\partial w}{r\partial \theta}\right), \quad \kappa_{ss} = \frac{\partial u_1}{\partial s}, \quad \kappa_{\theta\theta} = \frac{1}{r}\frac{\partial v_1}{\partial \theta} + \frac{\cos\varphi}{r} u_1,$$

$$\kappa_{s\theta} = \frac{1}{2}\left(\frac{\partial v_1}{\partial s} + \frac{1}{r}\frac{\partial u_1}{\partial \theta} - \frac{\cos\varphi}{r} v_1\right), \quad \varepsilon_{sz} = \frac{1}{2}\left(u_1 + \frac{\partial w}{\partial s}\right), \quad \kappa_{\theta z} = \frac{1}{2}\left(v_1 + \frac{1}{r}\frac{\partial w}{\partial \theta}\right), \tag{1.4}$$

where φ is the angle between the normal to the shell surface and the axis of revolution [20]. Considering the above hypotheses for the electric-flux density and integrating the expression

$$E_z^{(k)} = \frac{1}{\gamma_{33}^{(k)}} D_z^{(k)} - \frac{\gamma_{11}^{(k)}}{\gamma_{33}^{(k)}} \left[\varepsilon_{ss}^0 + \varepsilon_{\theta\theta}^0 + (\kappa_{ss} + \kappa_{\theta\theta}) z\right]$$

over the thickness coordinate z, we get

$$D_z^{(k)}(s,\theta) = -\frac{V_k - V_{k-1}}{H_1^{(k)}} + (\varepsilon_{ss}^0 + \varepsilon_{\theta\theta}^0)\frac{H_2^{(k)}}{H_1^{(k)}} + (\kappa_{ss} + \kappa_{\theta\theta})\frac{H_3^{(k)}}{H_1^{(k)}}, \tag{1.5}$$

where

$$H_1^{(k)} = \frac{a_k - a_{k-1}}{\gamma_{33}^{(k)}}, \quad H_2^{(k)} = \frac{\gamma_{11}^{(k)}}{\gamma_{33}^{(k)}} (a_k - a_{k-1}),$$

$$H_3^{(k)} = \frac{\gamma_{11}^{(k)}}{2\gamma_{33}^{(k)}}(a_k^2 - a_{k-1}^2), \qquad (k = 1, 2, 3). \tag{1.6}$$

With (1.5) and (1.6), the equations of state (1.2) become

$$\sigma_{ss}^{(k)} = A_{11}^{(k)}\varepsilon_{ss} + A_{12}^{(k)}\varepsilon_{\theta\theta} - \frac{\gamma_{11}^{(k)}}{\gamma_{33}^{(k)}}\left(-\frac{V_k - V_{k-1}}{H_1^{(k)}} + (\varepsilon_{ss}^0 + \varepsilon_{\theta\theta}^0)\frac{H_2^{(k)}}{H_1^{(k)}} + (\kappa_{ss} + \kappa_{\theta\theta})\frac{H_3^{(k)}}{H_1^{(k)}}\right),$$

$$\sigma_{\theta\theta}^{(k)} = A_{12}^{(k)}\varepsilon_{ss} + A_{11}^{(k)}\varepsilon_{\theta\theta} - \frac{\gamma_{11}^{(k)}}{\gamma_{33}^{(k)}}\left(-\frac{V_k - V_{k-1}}{H_1^{(k)}} + (\varepsilon_{ss}^0 + \varepsilon_{\theta\theta}^0)\frac{H_2^{(k)}}{H_1^{(k)}} + (\kappa_{ss} + \kappa_{\theta\theta})\frac{H_3^{(k)}}{H_1^{(k)}}\right),$$

$$\sigma_{s\theta}^{(k)} = 2G_{12}^{(k)}\varepsilon_{s\theta}, \qquad \sigma_{sz}^{(k)} = 2G_{13}^{(k)}\varepsilon_{sz}, \qquad \sigma_{\theta z}^{(k)} = 2G_{23}^{(k)}\varepsilon_{\theta z}, \tag{1.7}$$

where $A_{11}^{(k)} = B_{11}^{(k)} + \frac{\gamma_{11}^{(k)}\gamma_{11}^{(k)}}{\gamma_{33}^{(k)}}$, $A_{12}^{(k)} = B_{12}^{(k)} + \frac{\gamma_{11}^{(k)}\gamma_{11}^{(k)}}{\gamma_{33}^{(k)}}$.

To solve the three-dimensional problem of the dynamic behavior of inhomogeneous bodies of revolution under electromechanical loading, we use the following variational equation [4]:

$$\delta \mathrm{E} = 0, \tag{1.8}$$

where

$$\mathrm{E} = \frac{1}{2}\iiint\limits_V \left(c_{ijkl}\varepsilon_{ij}\varepsilon_{kl} - 2e_{ijk}E_i\varepsilon_{jk} - \mu_{ij}^s E_i E_j + \rho\frac{\partial^2 u_i}{\partial t^2}u_i + \zeta\frac{\partial u_i}{\partial t}u_i\right)dV - \iint\limits_S P_i u_i ds. \tag{1.9}$$

For simplicity, we will restrict the consideration to symmetric shells.

With the above hypotheses, the variational equation (1.8) is reduced to a nonlinear two-dimensional equation. Let us represent the two-dimensional functional as two components:

$$\mathrm{E} = \mathrm{E}_L + \mathrm{E}_{NL}, \tag{1.10}$$

where E_L is the linear component including the quadratic terms for displacements and their derivatives, and E_{NL} is a functional that includes terms of high order,

$$\mathrm{E}_L = \frac{1}{2}\iint\limits_F \left\{ C_{11}\left(\frac{\partial u_0}{\partial s} + \frac{w}{R_1}\right)^2 + 2C_{12}\left(\frac{\partial u_0}{\partial s} + \frac{w}{R_1}\right)\left(\frac{1}{r}\frac{\partial v_0}{\partial \theta} + \frac{\cos\varphi}{r}u_0 + \frac{w}{R_2}\right)\right.$$

$$+ C_{11}\left(\frac{1}{r}\frac{\partial v_0}{\partial \theta} + \frac{\cos\varphi}{r}u_0 + \frac{w}{R_2}\right)^2 + C_{44}\left(\frac{\partial v_0}{\partial s} + \frac{1}{r}\frac{\partial u_0}{\partial \theta} - \frac{\cos\varphi}{r}v_0\right)^2 + C_{55}\left(u_1 + \frac{\partial w}{\partial s} - \frac{u_0}{R_1}\right)^2$$

$$+ C_{55}\left(v_1 + \frac{1}{r}\frac{\partial w}{\partial \theta} - \frac{v_0}{R_2}\right)^2 + D_{11}\left(\frac{\partial u_1}{\partial s}\right)^2 + 2D_{12}\frac{\partial u_1}{\partial s}\left(\frac{1}{r}\frac{\partial v_1}{\partial \theta} + \frac{\cos\varphi}{r}u_1\right)$$

$$+ D_{11}\left(\frac{1}{r}\frac{\partial v_1}{\partial \theta} + \frac{\cos\varphi}{r}u_1\right)^2 + D_{44}\left(\frac{\partial v_1}{\partial s} + \frac{1}{r}\frac{\partial u_1}{\partial \theta} - \frac{\cos\varphi}{r}v_1\right)^2$$

$$\left. + \rho_1\left(\frac{\partial^2 u_0}{\partial t^2}u_0 + \frac{\partial^2 v_0}{\partial t^2}v_0 + \frac{\partial^2 w}{\partial t^2}w\right) + \zeta_1\left(\frac{\partial u_0}{\partial t}u_0 + \frac{\partial v_0}{\partial t}v_0 + \frac{\partial w}{\partial t}w\right)\right\} dF$$

$$+\iint_F \left\{ \frac{1}{2}\left[\left(\frac{\partial u_0}{\partial s} + \frac{w}{R_1} + \frac{1}{r}\frac{\partial v_0}{\partial \theta} + \frac{\cos\varphi}{r} u_0 + \frac{w}{R_2} \right) Q^0 \right.\right.$$

$$\left.\left. + \left(\frac{\partial u_1}{\partial s} + \frac{1}{r}\frac{\partial v_1}{\partial \theta} + \frac{\cos\varphi}{r} u_1 \right) Q^1 \right] - P_z w \right\} dF - \iint_{S_1} P_s u_0 \, ds_1 - \iint_{S_2} P_\theta v_0 \, ds_2, \tag{1.11}$$

$$E_{NL} = \frac{1}{2}\iint_F \left\{ C_{11}\left[\left(\frac{\partial u_0}{\partial s} + \frac{w}{R_1} \right)\left(\frac{\partial w}{\partial s} \right)^2 + \frac{1}{4}\left(\frac{\partial w}{\partial s} \right)^4 \right] + C_{12}\left[\left(\frac{\partial u_0}{\partial s} + \frac{w}{R_1} \right)\left(\frac{1}{r}\frac{\partial w}{\partial \theta} \right)^2 \right.\right.$$

$$\left. + \left(\frac{1}{r}\frac{\partial v_0}{\partial \theta} + \frac{\cos\varphi}{r} u_0 + \frac{w}{R_2} + \frac{1}{2}\left(\frac{1}{r}\frac{\partial w}{\partial \theta} \right)^2 \right)\left(\frac{\partial w}{\partial s} \right)^2 \right]$$

$$+ C_{11}\left[\left(\frac{1}{r}\frac{\partial v_0}{\partial \theta} + \frac{\cos\varphi}{r} u_0 + \frac{w}{R_2} \right)\left(\frac{1}{r}\frac{\partial w}{\partial \theta} \right)^2 + \frac{1}{4}\left(\frac{1}{r}\frac{\partial w}{\partial \theta} \right)^4 \right]$$

$$\left. + C_{44}\left[2\frac{1}{r}\frac{\partial w}{\partial s}\frac{\partial w}{\partial \theta}\left(\frac{\partial v_0}{\partial s} + \frac{1}{r}\frac{\partial u_0}{\partial \theta} - \frac{\cos\varphi}{r} v_0 \right) + \left(\frac{\partial w}{\partial s} \right)^2 \left(\frac{1}{r}\frac{\partial w}{\partial \theta} \right)^2 \right] \right\} dF,$$

$$dF = r ds d\theta, \tag{1.12}$$

where

$$C_{ij} = \sum_{k=1}^{3}\left(\int_{a_{k-1}}^{a_k} A_{ij}^{(k)} dz - \frac{H_2^{(k)} H_2^{(k)}}{H_1^{(k)}} \right), \quad D_{ij} = \sum_{k=1}^{3}\left(\int_{a_{k-1}}^{a_k} A_{ij}^{(k)} z^2 dz - \frac{H_3^{(k)} H_3^{(k)}}{H_1^{(k)}} \right), \quad (i, j = 1, 2),$$

$$Q^0 = \sum_{k=1}^{3} (V_k - V_{k-1}) \frac{H_2^{(k)}}{H_1^{(k)}}, \quad Q^1 = \sum_{k=1}^{3} (V_k - V_{k-1}) \frac{H_3^{(k)}}{H_1^{(k)}},$$

$$C_{44} = \sum_{k=1}^{3} \int_{a_{k-1}}^{a_k} G_{12}^{(k)} dz, \quad D_{44} = \sum_{k=1}^{3} \int_{a_{k-1}}^{a_k} G_{12}^{(k)} z^2 dz, \quad C_{55} = \sum_{k=1}^{3} \int_{a_{k-1}}^{a_k} G_{13}^{(k)} dz,$$

$$\rho_1 = \sum_{k=1}^{3} \int_{a_{k-1}}^{a_k} \rho^{(k)} dz, \quad \zeta_1 = \sum_{k=1}^{3} \int_{a_{k-1}}^{a_k} \zeta^{(k)} dz, \tag{1.13}$$

P_z, P_s, P_θ are the components of the surface load vector, $\rho^{(k)}$ and $\zeta^{(k)}$ are the density and the coefficient of viscous friction of the kth layer, respectively.

2. Finite-Element Method. To solve the variational problem, we will use the finite-element method with elements in the form of a twelve-node isoparametric quadrangle.

A cylindrical coordinate system (r, θ, s) is used as a global one combining all finite elements. Note that the meridional s and axial x coordinates are related by $ds = Adx$, $A = \sqrt{1 + (dr/dx)^2}$.

A normalized coordinate system (ξ, η) is used as a local one, in which the approximating functions are defined and integrated.

To approximate the deflection, its derivatives, tangential displacements, and rotation angles, cubical polynomials [13, 19] are used. The shell deflection is approximated within an element by Hermite bicubical polynomials:

$$w=\sum_{i=1}^{4}L_i(\xi,\eta)w_i+\sum_{i=1}^{4}L_{i+4}(\xi,\eta)\left(\frac{\partial w}{\partial s}\right)_i+\sum_{i=1}^{4}L_{i+8}(\xi,\eta)\left(\frac{1}{r}\frac{\partial w}{\partial\theta}\right)_i+\sum_{i=1}^{4}L_{i+12}(\xi,\eta)\left(\frac{\partial^2 w}{r\partial s\partial\theta}\right)_i, \tag{2.1}$$

where $w_i, \left(\frac{\partial w}{\partial s}\right)_i, \left(\frac{1}{r}\frac{\partial w}{\partial\theta}\right)_i, \left(\frac{\partial^2 w}{r\partial s\partial\theta}\right)_i$ are the amplitudes of the deflection and its derivatives at the corner points of the element, $L_i(\xi,\eta)$ are Hermite polynomials [13, 19].

The tangential components of the shell mid-surface and angles of rotation within an element are approximated by cubical polynomials:

$$u_0=\sum_{i=1}^{12}N_i(\xi,\eta)u_{0i}, \qquad v_0=\sum_{i=1}^{12}N_i(\xi,\eta)v_{0i},$$

$$u_1=\sum_{i=1}^{12}N_i(\xi,\eta)u_{1i}, \qquad v_1=\sum_{i=1}^{12}N_i(\xi,\eta)v_{1i}. \tag{2.2}$$

The explicit form of the polynomials $N_i(\xi,\eta)$ can be found in [13, 19].

In this case, the coordinates s, r, θ are related to the coordinates ξ, η as

$$s=\sum_{i=1}^{12}N_i(\xi,\eta)s_i, \qquad r=\sum_{i=1}^{12}N_i(\xi,\eta)r_i, \qquad \theta=\sum_{i=1}^{12}N_i(\xi,\eta)\theta_i, \tag{2.3}$$

where s_i, r_i, θ_i are the nodal values of the coordinates.

From relations (2.1)–(2.3) it follows that the finite element has 64 degrees of freedom: 8 degrees (w, $\partial w/\partial s$, $\partial w/(r\partial\theta)$, $\partial^2 w/(r\partial\theta\,\partial s)$, u_0, v_0, u_1, v_1) at each corner point and 4 degrees (u_0, v_0, u_1, v_1) at each node located on the sides of the quadrangle.

In [13, 19], the same finite element is used to solve static and dynamic problems for single-layer and multilayer shells. Here the numerical results on the stress–strain state of elastic and viscoelastic shells are compared with those obtained with analytical and other numerical methods. It should be noted that the usage of such approximation functions enables high accuracy of the solution for shells of different geometry.

It is assumed that the shell mid-surface is divided by N nodal points into M finite elements.

Representing the components of mechanical and electrical loads as

$$P=\sum_{i=1}^{12}N_i(\xi,\eta)P_i, \qquad V=\sum_{i=1}^{12}N_i(\xi,\eta)V_i$$

using the expressions for displacements (1.1) and strains (1.4), and the stationarity condition for functional (1.10) $\delta\text{E}=0$, we arrive at a system of nonlinear differential second-order equations for the deflection, its derivatives, tangential displacements, and angles of rotation [5, 19]:

$$\frac{\partial\text{E}}{\partial w_j}=\sum_{m=1}^{M}\frac{\partial\text{E}_m}{\partial w_j}=0, \quad \ldots, \quad \frac{\partial\text{E}}{\partial v_{1j}}=\sum_{m=1}^{M}\frac{\partial\text{E}_m}{\partial v_{1j}}=0. \tag{2.4}$$

The differentiation with respect to u_0, v_0, u_1, v_1 is carried out at all nodal points of the element, while the differentiation with respect to w, w^s, w^θ, $w^{s\theta}$ is performed at the corner points of the quadrangular element.

The system of differential equations (2.4) has the following matrix form:

$$[M]\frac{\partial^2 \boldsymbol{U}}{\partial t^2}+[C]\frac{\partial \boldsymbol{U}}{\partial t}+[K]\boldsymbol{U}+\boldsymbol{G}_{NL}(\boldsymbol{U})=\boldsymbol{Q}(t), \tag{2.5}$$

where $[M]$ is the mass matrix, $[C]$ is the loss matrix, $[K]$ is the stiffness matrix, $\boldsymbol{Q}(t)$ is the column vector of the external load, $\boldsymbol{U}$ is the column vector of the deflection and its derivatives, tangential displacements, and angles of rotation at corner points, $\boldsymbol{G}_{NL}(\boldsymbol{U})$ is the column vector whose components are obtained by differentiating the nonlinear component of functional (1.10). This vector includes elements with quadratic and cubic nonlinearity of the shell deflection.

The initial conditions are

$$\boldsymbol{U}=0, \quad \frac{\partial \boldsymbol{U}}{\partial t}=0 \quad \text{at} \quad t=0. \tag{2.6}$$

Let us represent the solution of the vector equation (2.5) under conditions (2.6) as a series describing the free vibrations of an electroelastic shell (energy dissipation being neglected):

$$\boldsymbol{U}(w,\ldots,v_1,t)=\sum_{n=1}^{\infty}\boldsymbol{W}_n(w,\ldots,v_1)f_n(t), \tag{2.7}$$

where $f_n(t)$ are functions of time to be determined.

The vibration modes are determined by solving the generalized eigenvalue problem

$$[K]\boldsymbol{W}_n-\omega_n^2[M]\boldsymbol{W}_n=0, \tag{2.8}$$

where $\boldsymbol{W}_n$ is the orthonormalized eigenvector satisfying the following conditions [1]:

$$\boldsymbol{W}_m^{\mathrm{T}}[M]\boldsymbol{W}_n=\begin{cases}0, & m\neq n,\\ 1, & m=n,\end{cases}$$

$$\boldsymbol{W}_m^{\mathrm{T}}[K]\boldsymbol{W}_n=\begin{cases}0, & m\neq n,\\ \omega_m^2, & m=n,\end{cases}$$

$$\boldsymbol{W}_m^{\mathrm{T}}[C]\boldsymbol{W}_n=\begin{cases}0, & m\neq n,\\ 2\omega_m\zeta_m, & m=n,\end{cases} \tag{2.9}$$

where ω_m is the circular frequency of free vibrations of the shell, ζ_m is the damping factor of the mth vibration mode.

Substituting (2.7) into (2.5), multiplying it by the transposed vector $\boldsymbol{W}_n^{\mathrm{T}}$, and allowing for (2.9), we obtain

$$\frac{\partial^2 f_n(t)}{\partial t^2}+2\omega_n\zeta_n\frac{\partial f_n(t)}{\partial t}+\omega_n^2 f_n(t)+\boldsymbol{W}_n^{\mathrm{T}}\boldsymbol{G}_{NL}(\boldsymbol{W}_n,f_n(t))=\boldsymbol{W}_n^{\mathrm{T}}\boldsymbol{W}\boldsymbol{Q}(t),$$

$$n=1,2,\ldots, \tag{2.10}$$

where, upon substitution of (2.7) into (2.7), the column vector $\boldsymbol{G}_{NL}=\boldsymbol{G}_{NL}(\boldsymbol{W}_n,f_n(t))$ becomes to be dependent on $\boldsymbol{W}_n$ and scalar function $f_n(t)$, which is reflected in the symbolic notation.

Calculating the components of the vector $\boldsymbol{G}_{NL}(\boldsymbol{W}_n,f_n(t))$ and multiplying the obtained vector and the transposed vector $\boldsymbol{W}_n^{\mathrm{T}}$ on the left-hand side, and grouping the coefficients of $(f_n(t))^2$ and $(f_n(t))^3$, we reduce the nonlinear differential second-order equation (2.10) to the form

$$\frac{d^2 f_n(t)}{dt^2}+2\omega_n\zeta_n\frac{df_n(t)}{dt}+\omega_n^2 f_n(t)+\beta_1 f_n^2(t)+\beta_2 f_n^3(t)=F_n(t),$$

$$n=1,2,\ldots. \tag{2.11}$$

Consider a shell undergoing single-frequency vibrations under harmonic loading $F_n(t)=F_{0n}\cos\Omega t$.

With the dimensionless parameters

$$\tau = \omega_n t, \qquad y = f_n \frac{\omega_n^2}{F_{0n}}, \qquad \eta_1 = \frac{\Omega}{\omega_n}, \qquad D = 2\zeta_n, \qquad \mu_1 = \beta_1 \frac{F_{0n}}{\omega_n^4}, \qquad \mu_2 = \beta_2 \frac{F_{0n}}{\omega_n^6}, \tag{2.12}$$

Eq. (2.11) becomes

$$\frac{d^2 y}{d\tau^2} + D\frac{dy}{d\tau} + y + \mu_1 y^2 + \mu_2 y^3 = \cos \eta_1 \tau. \tag{2.13}$$

Using the harmonic linearization method [2] and representing the solution as

$$y = A\cos\eta_1\tau + B\sin\eta_1\tau + Z, \tag{2.14}$$

we arrive at the following system of three nonlinear algebraic equations for the coefficients A, B, Z:

$$A(1-\eta_1^2) + DB\eta_1 + 2\mu_1 AZ + \mu_2\left(\frac{3}{4}A^3 + \frac{3}{4}AB^2 + 3AZ^2\right) = 1,$$

$$B(1-\eta_1^2) - DA\eta_1 + 2\mu_1 Bz + \mu_2\left(\frac{3}{4}B^3 + \frac{3}{4}A^2 B + 3BZ^2\right) = 0,$$

$$Z + \mu_1\left(\frac{X}{2} + Z^2\right) + \mu_2\left(\frac{3}{2}XZ + Z^3\right) = 0. \tag{2.15}$$

If the square of the amplitude X ($X = A^2 + B^2$) and the coefficient Z are considered unknown, the system of equations (2.15) is simplified:

$$\frac{9}{16}\mu_2^2 X^3 + \frac{3}{2}\mu_2(1-\eta_1^2)X^2 + [(1-\eta_1^2)^2 + D^2\eta_1^2]X + 9\mu_2^2 XZ^4 + 12\mu_1\mu_2 XZ^3$$

$$+\frac{9}{2}\mu_2 X^2 Z^2 + 6\mu_2(1-\eta_1^2)XZ^2 + 4\mu_1 XZ^2 + 3\mu_1\mu_2 X^2 Z + 4\mu_1(1-\eta_1^2)XZ = 1,$$

$$X\left(\frac{3}{2}\mu_2 Z + \frac{1}{2}\mu_1\right) + \mu_2 Z^3 + \mu_1 Z^2 + Z = 0. \tag{2.16}$$

Eliminating X from (2.16), we obtain an algebraic equation of the 9th degree for Z:

$$A_0 + A_1 Z + A_2 Z^2 + A_3 Z^3 + A_4 Z^4 + A_5 Z^5 + A_6 Z^6 + A_7 Z^7 + A_8 Z^8 + A_9 Z^9 = 0, \tag{2.17}$$

with the following coefficients:

$$A_0 = 2\mu_1^3, \qquad A_1 = 18\mu_1^2\mu_2 + 4\mu_1^2\mu_3, \qquad \mu_3 = (D\eta_1)^2 + (1-\eta_1^2)^2,$$

$$A_2 = 54\mu_1\mu_2^2 + (16\mu_1^3 - 12\mu_1\mu_2)(1-\eta_1^2) + 4\mu_3(\mu_1^3 + 6\mu_1\mu_2),$$

$$A_3 = 9\mu_2^2 - 24\mu_1^2\mu_2 + 4\mu_3(7\mu_1^2\mu_2 + 9\mu_2^2) + (1-\eta_1^2)(-36\mu_2^2 + 16\mu_1^4 + 96\mu_1^2\mu_2) + 54\mu_2^3 + 16\mu_1^4,$$

$$A_4 = -81\mu_1\mu_2^2 + 60\mu_1\mu_2^2\mu_3 + (1-\eta_1^2)(124\mu_1^3\mu_2 + 192\mu_1\mu_2^2) + 96\mu_1^3\mu_2 + 16\mu_1^5,$$

$$A_5 = -81\mu_2^3 + 231\mu_1^2\mu_2^2 + (1-\eta_1^2)(384\mu_1^2\mu_2^2 + 144\mu_2^3) + 136\mu_1^4\mu_2 + 36\mu_2^3\mu_3,$$

$$A_6 = 270\mu_1\mu_2^3 + 420\mu_1\mu_2^3(1-\eta_1^2) + 465\mu_1^3\mu_2^2,$$

$$A_7 = 135\mu_2^4 + 795\mu_1^2\mu_2^3 + 180\mu_2^4(1-\eta_1^2), \qquad A_8 = 675\mu_1\mu_2^4, \qquad A_9 = 225\mu_2^5.$$

Finding the real roots of polynomial (2.17), we can find the square of the amplitude X and the coefficients A and B:

$$X=-2\frac{\mu_2 Z^3+\mu_1 Z^2+Z}{3\mu_2 Z+\mu_1},\qquad A=\frac{3}{4}\mu_2 X^2+[(1-\eta_1)+2\mu_1 Z+3\mu_2]X,\qquad B=XD\eta_1.$$

3. Analytical-and-Numerical Method for Solving the Problem of the Nonlinear Vibrations of a Hinged Three-Layer Viscoelectroelastic Cylindrical Panel. Nonlinear problems of the dynamic behavior of a closed cylindrical shell and hinged cylindrical panel are solved analytically using double trigonometric series. These solutions can be regarded as standard in the development of numerical methods.

Let us consider the problem of the nonlinear vibrations of a symmetric cylindrical sandwich panel with radius R under uniformly distributed pressure $P_z=P_0\cos\Omega t$. A potential is applied to the electroded surfaces of the panel. In problems of the bending vibrations of plates and shells, inertial forces acting along the normal to the mid-surface dominate. Neglecting the inertial forces for the tangential and shear components, we arrive at the following simplified variational equation:

$$\delta \mathrm{E}=\delta(\mathrm{E}_L+\mathrm{E}_{NL})=0, \tag{3.1}$$

$$\begin{aligned}\mathrm{E}_L=\frac{1}{2}\iint_F\Bigg\{&C_{11}\left(\frac{\partial u_0}{\partial s}\right)^2+2C_{12}\left(\frac{\partial u_0}{\partial s}\right)\left(\frac{1}{r}\frac{\partial v_0}{\partial\theta}+\frac{w}{R}\right)\\
&+C_{11}\left(\frac{1}{r}\frac{\partial v_0}{\partial\theta}+\frac{w}{R}\right)^2+C_{44}\left(\frac{\partial v_0}{\partial s}+\frac{1}{r}\frac{\partial u_0}{\partial\theta}\right)^2+C_{55}\left(u_1+\frac{\partial w}{\partial s}\right)^2\\
&+C_{55}\left(v_1+\frac{1}{r}\frac{\partial w}{\partial\theta}\right)^2+D_{11}\left(\frac{\partial u_1}{\partial s}\right)^2+2D_{12}\frac{\partial u_1}{\partial s}\left(\frac{1}{r}\frac{\partial v_1}{\partial\theta}\right)\\
&+D_{11}\left(\frac{1}{r}\frac{\partial v_1}{\partial\theta}\right)^2+D_{44}\left(\frac{\partial v_1}{\partial s}+\frac{1}{r}\frac{\partial u_1}{\partial\theta}\right)^2+\rho_1\frac{\partial^2 w}{\partial t^2}w+\zeta_1\left(\frac{\partial w}{\partial t}w\right)\Bigg\}dF\\
&+\iint_F\left\{\frac{1}{2}\left[\left(\frac{\partial u_0}{\partial s}+\frac{1}{r}\frac{\partial v_0}{\partial\theta}+\frac{w}{R}\right)Q^0+\left(\frac{\partial u_1}{\partial s}+\frac{1}{r}\frac{\partial v_1}{\partial\theta}\right)Q^1\right]-P_z w\right\}dF,\end{aligned} \tag{3.2}$$

$$\begin{aligned}\mathrm{E}_{NL}=\frac{1}{2}\iint_F\Bigg\{&C_{11}\left[\frac{\partial u_0}{\partial s}\left(\frac{\partial w}{\partial s}\right)^2+\frac{1}{4}\left(\frac{\partial w}{\partial s}\right)^4\right]+C_{12}\left[\frac{\partial u_0}{\partial s}\left(\frac{1}{r}\frac{\partial w}{\partial\theta}\right)^2\right.\\
&\left.+\left(\frac{1}{r}\frac{\partial v_0}{\partial\theta}+\frac{w}{R}\right)\left(\frac{\partial w}{\partial s}\right)^2+\frac{1}{2}\left(\frac{\partial w}{\partial s}\right)^2\left(\frac{1}{r}\frac{\partial w}{\partial\theta}\right)^2\right]+C_{11}\left[\left(\frac{1}{r}\frac{\partial v_0}{\partial\theta}++\frac{w}{R}\right)\left(\frac{1}{r}\frac{\partial w}{\partial\theta}\right)^2+\frac{1}{4}\left(\frac{1}{r}\frac{\partial w}{\partial\theta}\right)^4\right]\\
&+C_{44}\left[2\left(\frac{\partial v_0}{\partial s}+\frac{1}{r}\frac{\partial u_0}{\partial\theta}\right)\left(\frac{\partial w}{\partial s}\frac{1}{r}\frac{\partial w}{\partial\theta}\right)+\left(\frac{\partial w}{\partial s}\right)^2\left(\frac{1}{r}\frac{\partial w}{\partial\theta}\right)^2\right]\Bigg\}dF,\qquad dF=rdsd\theta.\end{aligned}$$

Denoting $x=s\,(0\le x\le a)$ and $y=R\theta\,(0\le y\le b)$, we reduce the problem to the variational equation (3.1) subject to the initial conditions

$$w=0,\qquad \frac{\partial w}{\partial t}=0\quad\text{at}\quad t=0 \tag{3.3}$$

and the boundary conditions

$$w=0,\quad \frac{\partial^2 w}{\partial x^2}=0,\quad v_0=0,\quad v_1=0\quad \text{at}\quad x=0,\quad x=a,$$

$$w=0,\quad \frac{\partial^2 w}{\partial y^2}=0,\quad u_0=0,\quad u_1=0\quad \text{at}\quad y=0,\quad y=b. \tag{3.4}$$

Considering the boundary conditions (3.4), we seek the solution in the form of a double trigonometric series:

$$w=\sum_{m=1}^{\infty}\sum_{n=1}^{\infty} w_{mn}(t)\sin(k_m x)\sin(p_n y),$$

$$u_0=\sum_{m=1}^{\infty}\sum_{n=1}^{\infty} u_{mn}^0(t)\cos(k_m x)\sin(p_n y),$$

$$v_0=\sum_{m=1}^{\infty}\sum_{n=1}^{\infty} v_{mn}^0(t)\sin(k_m x)\cos(p_n y),$$

$$u_1=\sum_{m=1}^{\infty}\sum_{n=1}^{\infty} u_{mn}^1(t)\cos(k_m x)\sin(p_n y),$$

$$v_1=\sum_{m=1}^{\infty}\sum_{n=1}^{\infty} v_{mn}^1(t)\sin(k_m x)\cos(p_n y), \tag{3.5}$$

where $k_m=\frac{m\pi}{a}$, $p_n=\frac{n\pi}{b}$, $(m,n=1,2,3,\dots)$.

Let us expand the components of mechanical and electrical loads into series of trigonometric functions:

$$P_0=\sum_{m=1}^{\infty}\sum_{n=1}^{\infty} P_{mn}\sin(k_m x)\sin(p_n y),$$

$$V_k-V_{k-1}=\sum_{m=1}^{\infty}\sum_{n=1}^{\infty} V_{mn}^k\sin(k_m x)\sin(p_n y),$$

$$P_{mn}=\frac{16P_0}{abk_m p_n},\qquad V_{mn}^k=\frac{16(V_k-V_{k-1})}{abk_m p_n}. \tag{3.6}$$

Using expressions (3.5), (3.6) and condition (3.1), we obtain a system of equations for the coefficients of the series:

$$(C_{11}k_m^2+C_{44}p_n^2)u_{mn}^0+(C_{12}+C_{44})k_m p_n v_{mn}^0-C_{12}\frac{k_m}{R}w_{mn}$$

$$-\frac{16}{9ab}\left[(C_{11}\frac{k_m^2}{p_n}+(C_{12}-C_{44})p_n\right]w_{mn}^2-Q_{mn}^0 k_m=0,$$

$$(C_{12}+C_{44})k_m p_n u_{mn}^0+(C_{11}p_n^2+C_{44}k_m^2)v_{mn}^0-C_{12}\frac{p_n}{R}w_{mn}$$

$$-\frac{16}{9ab}\left[(C_{11}\frac{p_n^2}{k_m}+(C_{12}-C_{44})k_m\right]w_{mn}^2-Q_{mn}^0 p_n=0,$$

$$(D_{11}k_m^2 + D_{44}p_n^2 + C_{55})u_{mn}^1 + (D_{12} + D_{44})k_m p_n v_{mn}^1 + C_{55}k_m w_{mn} - Q_{mn}^1 k_m = 0,$$

$$(D_{12} + D_{44})k_m p_n u_{mn}^1 + (D_{11}p_n^2 + D_{44}k_m^2 + C_{55})v_{mn}^1 + C_{55}p_n w_{mn} - Q_{mn}^1 p_n = 0,$$

$$\rho_1 \frac{\partial^2 w_{mn}}{\partial t^2} + \zeta_{mn} \frac{\partial w_{mn}}{\partial t} + \left[C_{11}\frac{1}{R^2} + C_{55}(p_n^2 + k_m^2)\right]w_{mn} - C_{12}k_m \frac{1}{R}u_{mn}^0 - C_{11}p_n \frac{1}{R}v_{mn}^0$$

$$+ C_{55}k_m u_{mn}^1 + C_{55}p_n v_{mn}^1 + \frac{32}{9abk_m p_n}\Big[-C_{11}(k_m^3 u_{mn}^0 + p_n^2 v_{mn}^0)$$

$$+ (C_{44} - C_{12})(k_m p_n^2 u_{mn}^0 + k_m^2 p_n v_{mn}^0)\Big]w_{mn} + \frac{16}{3abk_m p_n}(C_{12}k_m^2 + C_{11}p_n^2)\frac{w_{mn}^2}{R}$$

$$+ \frac{1}{32}C_{11}(9k_m^4 + 2k_m^2 p_n^2 + 9p_n^4)w_{mn}^3 - Q_{mn}^0 \frac{1}{R} - P_{mn} = 0, \qquad (3.7)$$

where ζ_{mn} is the coefficient of viscous friction; $Q_{mn}^0 = \frac{1}{2}\sum_{k=1}^{3} V_{mn}^k \frac{H_2^{(k)}}{H_1^{(k)}}, Q_{mn}^1 = \frac{1}{2}\sum_{k=1}^{3} V_{mn}^k \frac{H_3^{(k)}}{H_1^{(k)}}.$

The solutions of the first four equations appearing in (3.7) can be represented as

$$u_{mn}^0 = S_1 \frac{w_{mn}}{R} + Q_1 w_{mn}^2 + Q_{mn}^0 \frac{k_m}{C_{11}(k_m^2 + p_n^2)},$$

$$v_{mn}^0 = S_2 \frac{w_{mn}}{R} + Q_2 w_{mn}^2 + Q_{mn}^0 \frac{p_n}{C_{11}(k_m^2 + p_n^2)},$$

$$u_{mn}^1 = -\frac{C_{55}k_m}{D_{11}(k_m^2 + p_n^2) + C_{55}} w_{mn} + Q_{mn}^1 \frac{k_m}{D_{11}(k_m^2 + p_n^2) + C_{55}},$$

$$v_{mn}^1 = -\frac{C_{55}p_n}{D_{11}(k_m^2 + p_n^2) + C_{55}} w_{mn} + Q_{mn}^1 \frac{p_n}{D_{11}(k_m^2 + p_n^2) + C_{55}}, \qquad (3.8)$$

where

$$S_1 = \frac{k_m(C_{12}k_m^2 - C_{11}p_n^2)}{C_{11}(k_m^2 + p_n^2)^2}, \qquad S_2 = \frac{p_n[C_{11}(p_n^2 + k_m^2) - (C_{11} + C_{12})k_m^2]}{C_{11}(k_m^2 + p_n^2)^2},$$

$$Q_1 = \frac{16}{9abk_m p_n} \frac{(5C_{12} + 4C_{44})k_m^3 p_n^2 - 2C_{11}k_m p_n^4 + C_{11}k_m^5}{C_{11}(k_m^2 + p_n^2)^2},$$

$$Q_2 = \frac{16}{9abk_m p_n} \frac{(5C_{12} + 4C_{44})k_m^2 p_n^3 - 2C_{11}k_m^4 p_n + C_{11}p_n^5}{C_{11}(k_m^2 + p_n^2)^2}.$$

Substituting expressions (3.8) for $u_{mn}^0, v_{mn}^0, u_{mn}^1, v_{mn}^1$ into the fifth equation of system (3.7), we arrive at the nonlinear second-order differential equation

$$\frac{d^2 w_{mn}}{dt^2} + 2\zeta_{mn}^* \frac{dw_{mn}}{dt} + \omega_{mn}^2 w_{mn} + \beta_1 (w_{mn})^2 + \beta_2 (w_{mn})^3 = \frac{1}{\rho_1} P_{mn}$$

$$+\frac{1}{\rho_1}\left[\frac{1}{R}Q^0_{mn}\,\frac{(C_{12}k_m^2+C_{11}p_n^2)}{C_{11}(k_m^2+p_n^2)^2}+Q^1_{mn}\,\frac{C_{55}(p_n^2+k_m^2)^2}{D_{11}(k_m^2+p_n^2)+C_{55}}\right], \tag{3.9}$$

where

$$\omega_{mn}^2=\left[\frac{C_{55}D_{11}(k_m^2+p_n^2)^2}{D_{11}(k_m^2+p_n^2)+C_{55}}+\frac{(C_{11}^2-C_{12}^2)^2k_m^4}{C_{11}R^2(k_m^2+p_n^2)^2}\right]\frac{1}{\rho_1},\qquad \zeta^*_{mn}=\frac{\zeta_{mn}}{2\rho_1},$$

$$\beta_1=\frac{1}{\rho_1 R}\left\{\frac{16}{3abk_m p_n}(C_{12}k_m^2+C_{11}p_n^2)-C_{12}k_mQ_1-C_{11}p_nQ_2\right.$$

$$\left.+\frac{32}{9abk_m p_n}[(C_{44}-C_{12})(k_m p_n^2S_1+k_m^2p_nS_2)-C_{11}(k_m^3S_1+p_n^3S_2)]\right\},$$

$$\beta_2=\frac{C_{11}}{64\rho_1}(9k_m^4+2k_m^2p_n^2+9p_n^4)$$

$$+\frac{32}{9abk_m p_n\rho_1}[(C_{44}-C_{12})(k_m p_n^2Q_1+k_m^2p_nQ_2)-C_{11}(k_m^3Q_1+p_n^3Q_2)],$$

ζ^*_{mn} is the damping factor.

Since the mechanical loading and electrical potential are periodic time functions, Eq. (3.9) can be solved with the method described in Sec. 2.

4. Technique of Analysis of the Temperature Field. The analysis of the thermomechanical state of the above viscoelastic piezoelectric shells of revolution under electromechanical loading is reduced to the sequential solution of the problem of the forced vibrations of these shells and the problem of nonstationary heat conduction to determine the dissipative heating temperature.

To determine this temperature, we use the FEM with the same mesh of finite elements as in the case of the dynamic problem considered above (Sec. 2). We will use the following three-dimensional variational heat-conduction equation [4]:

$$\delta I=0, \tag{4.1}$$

where

$$I=\frac{1}{2}\iiint_V\left\{\lambda^{(k)}\left[\left(\frac{\partial T^{(k)}}{\partial z}\right)^2+\left(\frac{\partial T^{(k)}}{\partial r}\right)^2+\left(\frac{1}{r}\frac{\partial T^{(k)}}{\partial\theta}\right)^2\right]+2C^{(k)}\rho^{(k)}\frac{\partial T^{(k)}}{\partial t}T^{(k)}-2D^{(k)}T^{(k)}\right\}dV$$

$$+\frac{1}{2}\iint_\Sigma\alpha_T(T^{(k)}-2\theta_c)T^{(k)}d\Sigma, \tag{4.2}$$

where V is the volume of the body of revolution bounded by the surface Σ, $\lambda^{(k)}$ is heat conductivity, $C^{(k)}$ is the specific heat capacity, $\rho^{(k)}$ is the density of the material of the kth layer, α_T is the coefficient of heat transfer from the body surface to the environment of temperature θ_c.

For the vibration heating problem, the function of heat sources $D^{(k)}$ for the kth layer appearing in (4.2) is equal to the cycle-average dissipative function, which is defined in the terms of the complex physical and mechanical characteristics of the material, the complex components of stress tensor $\sigma_{ij}^{(k)}=\sigma_{ij}'^{(k)}+i\sigma_{ij}''^{(k)}$, strain tensor $\varepsilon_{ij}^{(k)}=\varepsilon_{ij}'^{(k)}+i\varepsilon_{ij}''^{(k)}$, electric strength $E_j^{(k)}=E_j'^{(k)}+iE_j''^{(k)}$, and the electric-flux density $D_j^{(k)}=D_j'^{(k)}+iD_j''^{(k)}$, where

$$D^{(k)} = \frac{\omega}{2}(\sigma''^{(k)}_{ij}\varepsilon'^{(k)}_{ij} - \sigma'^{(k)}_{ij}\varepsilon''^{(k)}_{ij} + E''^{(k)}_{j}D'^{(k)}_{j} - E'^{(k)}_{j}D''^{(k)}_{j}). \quad (4.3)$$

Various methods for determining temperatures fields in plates and shells are presented in [7, 18]. In many cases, the three-dimensional heat-conduction problem is reduced to a sequence of two-dimensional problems (Sec. 2). To this end, we represent the temperature as a series:

$$T^{(k)}(s,\theta,z,t) = \sum_{i=0}^{m} T_i^{(k)}(s,\theta,t)p_i(z), \quad (4.4)$$

where $T_i^{(k)}(s,\theta,t)$ are unknown functions characterizing the temperature field on the coordinate surface; $p_i(z)$ are given functions of distribution of the temperature field over the shell thickness. These functions satisfy the conditions of perfect thermal contact between the layers and allow describing the temperature over the thickness of each layer as a polynomial of arbitrary *m*th degree. In solving many practical problems, it is possible to retain three terms in series (4.4). Then, it follows from (4.4) that the temperature of the *k*th layer is approximated by a square polynomial in z ($m = 2$).

Using the standard FEM procedure and assuming that the time derivative dT / dt is not varied, we arrive at a system of $3N$ linear differential equations for the nodal values T_i. To solve the system of ordinary differential equations, we use the finite-difference method with time approximation $dT_i / dt \approx \left(T_i(t+\Delta t) - T_i(t)\right) / \Delta t$. To find the temperature T_i at $t + \Delta t$, we use the equation with unknowns written for the same instant of time. This allows using an implicit scheme for the solving the problem with respect to time, namely, to derive a system of $3N$ linear algebraic equations to determine the temperature at nodal points [7, 18].

5. Analysis of Numerical Results. The developed technique of analyzing the nonlinear vibrations of laminated shells with transverse shear strains was validated by comparing the numerical results obtained with the analytical-and-numerical approach and with the finite-element method.

We consider, as an example, the problem for a three-layer hinged cylindrical panel of constant thickness whose middle layer is passive and viscoelastic. The panel is acted upon by uniformly distributed mechanical pressure $P_z = P_0 \cos\Omega t$. The outer layers of the panel are made of a piezoelectric viscoelastic material. The electroded surfaces are free of potential.

The middle layer of the panel is made of an aluminum alloy with the following characteristics:

$$E = E' + iE'' = (7.3 + 0.0016i)\times 10^{10}\ \text{N/m}^2, \quad \nu = 0.34, \quad \rho = 0.28\times 10^4\ \text{kg/m}^3.$$

The piezoelectric layers are made of PZT (EC-65) piezoceramic with the following complex physical-and-mechanical characteristics [26]:

$$s^E_{ij} = s'_{ij} + is''_{ij}, \quad d_{ij} = d'_{ij} + id''_{ij}, \quad \varepsilon^T_{ij} = \varepsilon'_{ij} + i\varepsilon''_{ij},$$

where

$$s'_{11} = 0.171\times 10^{-10}\ \text{m}^2/\text{N}, \quad s'_{12} = -0.58\times 10^{-11}\ \text{m}^2/\text{N}, \quad s'_{13} = -0.91\times 10^{-11}\ \text{m}^2/\text{N},$$

$$s'_{33} = 0.184\times 10^{-10}\ \text{m}^2/\text{N}, \quad s'_{55} = 0.460\times 10^{-10}\ \text{m}^2/\text{N}, \quad d'_{31} = -189.7\times 10^{-12}\ \text{C/m}^2,$$

$$d'_{33} = 357\times 10^{-12}\ \text{C/m}^2, \quad d'_{15} = 609\times 10^{-12}\ \text{C/m}^2, \quad \varepsilon'_{11} = 0.20541\times 10^{-7}\ \text{F/m},$$

$$\varepsilon'_{33} = 0.14803\times 10^{-7}\ \text{F/m}, \quad s''_{11} = -0.2\times 10^{-12}\ \text{m}^2/\text{N}, \quad s''_{12} = 0.1\times 10^{-12}\ \text{m}^2/\text{N},$$

$$s''_{13} = 0.2\times 10^{-12}\ \text{m}^2/\text{N}, \quad s''_{33} = -0.4\times 10^{-12}\ \text{m}^2/\text{N}, \quad s''_{55} = -5.6\times 10^{-12}\ \text{m}^2/\text{N},$$

$$d''_{31} = -4.8\times 10^{-12}\ \text{C/m}^2, \quad d''_{33} = -14.7\times 10^{-12}\ \text{C/m}^2, \quad d''_{15} = -253.6\times 10^{-12}\ \text{C/m}^2,$$

$$\varepsilon''_{11} = -11270\times 10^{-12}\ \text{F/m}, \quad \varepsilon''_{33} = -342\times 10^{-12}\ \text{F/m},$$

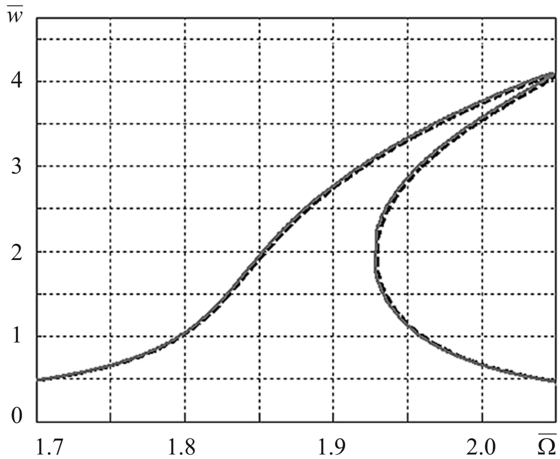

Fig. 1

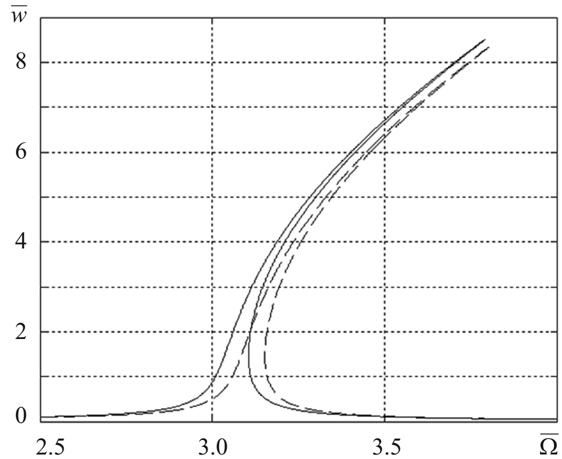

Fig. 2

where $\rho = 0.75\times 10^4$ kg/m^3 is the density of piezoceramic.

The parameters s_{ij}^E, d_{ij}, ε_{ij}^T are related to the physical-and-mechanical characteristics c_{ij}^E, e_{ij}, μ_{ij}^S of the piezomaterial by the transformation formulas [6].

The numerical results presented below correspond to the following shells: a thin-walled shell ($H / R = 0.01$) with parameters $H = 0.001$ m, $h_1 = h_3 = 0.00025$ m, $h_2 = 0.0005$ m, $R = 0.1$ m, $a = L = 0.1$ m, $b = R\theta = 0.1$ m; medium-thickness shell ($H / R = 0.1$) with parameters $H = 0.01$ m, $h_1 = h_3 = 0.0025$ m, $h_2 = 0.005$ m, $R = 0.1$ m, $a = L = 0.1$ m, $b = R\theta = 0.1$ m; and very thick shell ($H / R = 0.2$) with parameters $H = 0.01$ m, $h_1 = h_3 = 0.005$ m, $h_2 = 0.01$ m, $R = 0.1$ m, $a = L = 0.1$ m, $b = R\theta = 0.1$ m.

The damping factor of each vibration mode ζ_n is strongly dependent on the physical-and-mechanical properties of the material, the thickness of layers, and the frequency of free vibrations. Depending on the values of these parameters, it can vary from 0.0001 to 0.5.

Here, using the technique [1] and allowing for the viscoelectroelastic properties of the layers, we have determined the loss matrix. Next, allowing for the orthogonality of the eigenfunctions, we have calculated the damping factor for each vibration mode.

In solving the problem with the finite-element method, the quarter of the shell surface was divided into 25 quadrangular finite elements with 456 nodal points.

The figures presented below show the deflection amplitudes at the middle point $(a / 2, b / 2)$ of the panel at the resonant frequency at which the deflection amplitude is maximum.

For cylindrical panels with different thicknesses ($H / R = 0.01$, $H / R = 0.1$, $H / R = 0.2$), we have compared the results obtained with the classic Kirchhoff–Love theory and the approach [20] with those obtained with the refined Timoshenko-type theory.

In Figs. 1–5, $\overline{\Omega}$ and $\overline{w}$ denote the excitation frequency and the deflection amplitude at the middle point of the panel: $\Omega = \overline{\Omega}\times 10^4$ rad/sec, $|w(a / 2, b / 2)| = \overline{w}\times 10^{-3}$ m.

Figure 1 shows the variation in the deflection amplitude of the panel with $H / R = 0.01$ at the first resonant frequency $\omega_1 = 1.88186\times 10^4$ rad/sec for the damping factor of the first mode $\zeta_1 = 0.01$. The mechanical loading is defined by $P_0 = 0.1$MPa. The solid line represents the results obtained with the FEM, while the dashed line to the results obtained analytically. Note that the results obtained for the same panel using the Timoshenko theory with either the FEM or analytically are similar to those found with the classical theory.

For other values of the thicknesses, deviations are different. As an example, Fig. 2 demonstrates the behavior of the deflection amplitude at the first resonant frequency $\omega_1 = 3.05328\times 10^4$ rad/sec for the panel with $H / R = 0.1$ under mechanical loading $P_0 = 0.01$ MPa for the damping factor $\zeta = 0.0016$.

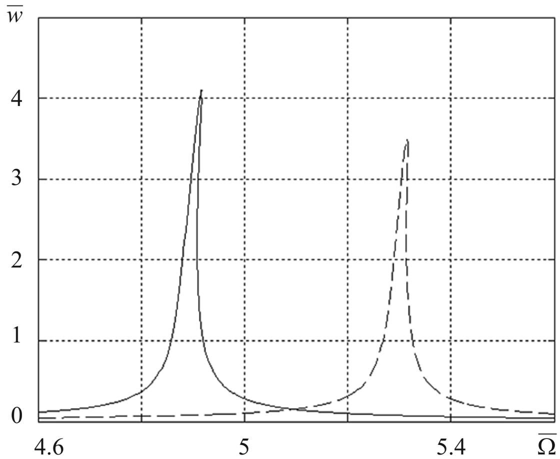

Fig. 3

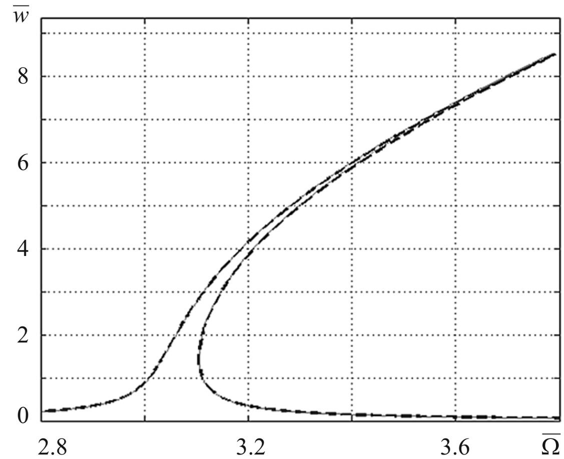

Fig. 4

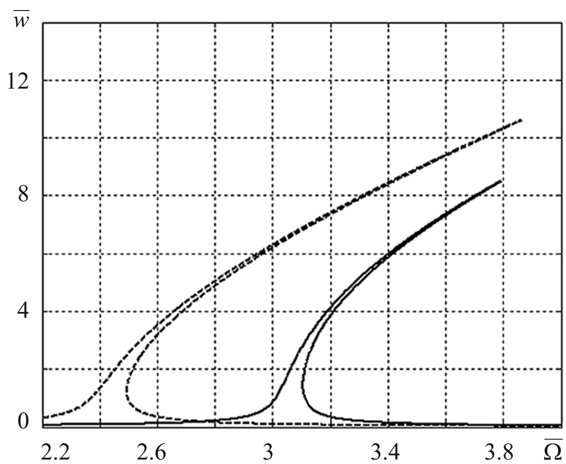

Fig. 5

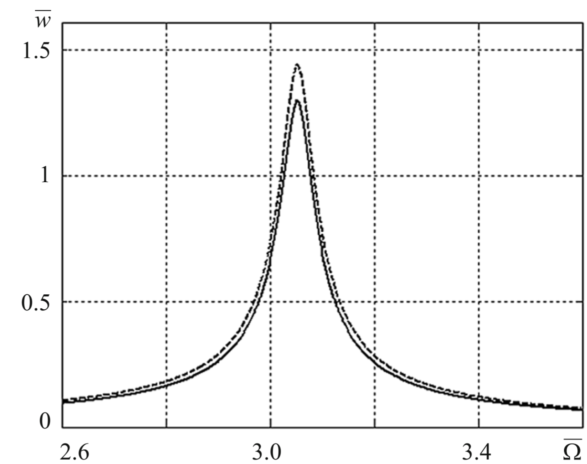

Fig. 6

Figure 3 illustrates the behavior of the deflection amplitude for a very thick panel with $H / R = 0.2$ under the same loading. An analytical method has been used. The solid lines in Figs. 2 and 3 refer to Timoshenko's theory, while the dashed line to the Kirchhoff–Love classical theory.

Figures 2 and 3 indicate that allowing for the transverse shear strains reduces the resonant frequency and increases the deflection amplitude. Hence, refined hypotheses should be applied to moderately thin panels.

Figure 4 shows the variation in the deflection amplitude at the first resonant frequency $\omega_1 = 3.05328 \times 10^4$ rad/sec under mechanical loading $P_0 = 0.01$ MPa for $H / R = 0.1$ and $\zeta_1 = 0.0016$ (the solid line corresponds to the finite element method, and the dashed line to the analytical method). It can be seen that the results obtained with these approaches are in good agreement, which is indicative of high accuracy of finite element software.

For comparison, Fig. 5 demonstrates the deflection amplitude at the first resonant frequency calculated with the analytical approach based on Timoshenko's theory ($P_0 = 0.01$ MPa, $\zeta_1 = 0.0016$) for $H / R = 0.1$ (solid line) and $H / R = 10$ (dashed line). In the latter case, the solution is similar to that for a plate.

From Figs. 2–5 it follows that the influence of the geometrical nonlinearity on the frequency dependence of the deflection amplitude is strongly dependent on the cylindrical panel and the viscoelastic characteristics of its material.

To validate the method of analyzing the nonlinear transverse vibrations of thin-walled elements under electrical loading, we have analyzed vibrations of the above panel with outer electrodes subject to a potential with an amplitude of 360 V, and the inner electrode subject to a zero potential.

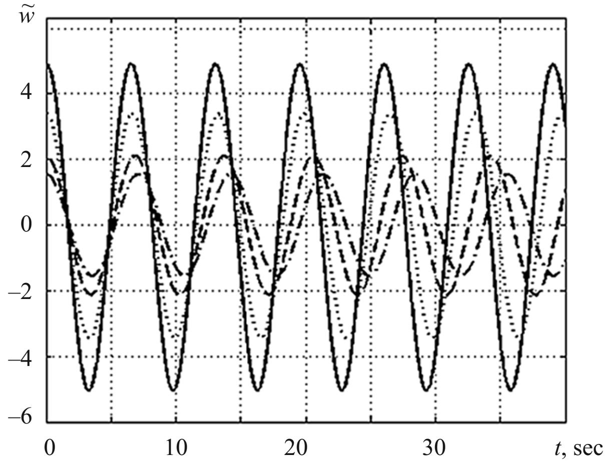

Fig. 7

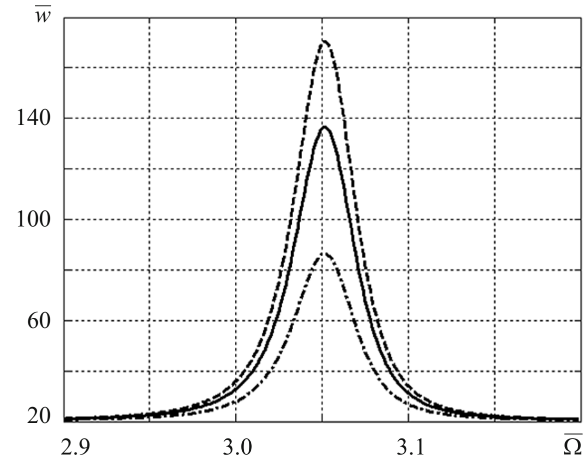

Fig. 8

For comparison, Fig. 6 presents the results obtained with the finite-element method (solid line) and analytical method (dashed line), described in Sec. 3, for a panel with $H/R = 0.1$ and $\zeta_1 = 0.01$ at the first resonant frequency. Here $\overline{\Omega}$ and $\overline{w}$ are the excitation frequency and the deflection amplitude at the middle point of the panel: $\Omega = \overline{\Omega} \times 10^4$ rad/sec, $|w(a/2, b/2)| = \overline{w} \times 10^{-4}$ m.

Figure 7 shows the dynamic variation of the defection amplitude $w(a/2, b/2) = \tilde{w} \times 10^{-4}$ m at the middle point of the panel with $H/R = 0.1$ under mechanical loading $P_0 = 0.01$ MPa for the damping factor $\zeta_1 = 0.0016$ and the following values of the circular excitation frequency: $\Omega = 0.27 \times 10^5$ rad/sec (dash-and-dot line), $\Omega = 0.28 \times 10^5$ rad/sec (dashed line), $\Omega = 0.29 \times 10^5$ rad/sec (dotted line), and $\Omega = 0.295 \times 10^5$ rad/sec (solid line). These results have been obtained analytically.

Using the technique of solving the heat conduction problem presented in the previous section, we have analyzed the dissipative heating temperature field of a panel of medium thickness ($H/R = 0.1$) under electrical loading (some electric potential applied to the outer electrode and zero potential applied to the inner electrode).

To determine the dissipative function, we used the complex characteristics of PZT (EC-65) piezoceramic and aluminum and the coefficients A, B, Z found numerically for calculating the complex components of the strain and stress tensors.

To determine the temperature field, we used the finite-element method with the following heat-physical characteristics and environmental temperature: heat-conduction coefficient $\lambda^{(1)} = \lambda^{(3)} = 1.25$ W/(m°C) for the piezoceramic layers and $\lambda^{(2)} =$ 200 W/(m°C) for the aluminum layer, the thermal diffusivity coefficients $a^{(1)} = a^{(3)} = 0.4 \times 10^{-6}$ m^2/sec and $a^{(2)} = 0.1 \times 10^{-5}$ m^2/sec, respectively, the heat-transfer coefficient $\alpha_T = 20$ W/(m^2·°C), environmental temperature $\theta_c = 20$ °C.

Figure 8 demonstrates the dependence of the temperature of the panel at the middle point $(a/2, b/2)$ on the angular frequency $\Omega = \overline{\Omega} \times 10^4$ rad/sec at the first resonant frequency $\omega_1 = 3.05328 \times 10^4$ rad/sec for the following amplitudes of the electrical potential on the outer surfaces of the cylindrical panel: 60 V (dash-and-dot line), 70 V (solid line), and 75 V (dashed line).

The numerical results show that allowing for geometric nonlinearity strongly affects the distribution of temperature at the first resonant frequency.

Conclusions. We have developed a combined numerical-and-analytical technique for analyzing the forced geometrically nonlinear vibrations of layered viscoelastic piezoelectrical shells of revolution and shell-like structural members under electromechanical loading with allowance for the transverse shear strains and dissipative heating. The numerical approach has been tested by solving the problem of the vibrations of a hinged viscoelectroelastic cylindrical panel at the first resonant frequency. The results calculated for the panels of different thicknesses have been compared to those obtained using the classical Kirchhoff–Love hypotheses and refined Timoshenko-type hypotheses. The numerical simulation has shown that allowing for the transverse shear strains decreases the resonant frequency. In studying the forced geometrically nonlinear vibrations of moderately thin panels, refined hypotheses should be applied. We have analyzed the dissipative heating temperature of the viscoelectroelastic cylindrical panel under electrical loading.

REFERENCES

1. K. J. Bathe and E. L. Wilson, *Numerical Methods in Finite Element Analysis*, Prentice-Hall, Englewood Cliffs, New Jersey (1976).
2. V. V. Bolotin, *Dynamical Stability of Elastic Systems* [in Russian], Gostekhizdat, Moscow (1956).
3. K. Washizu, *Variational Methods in Elasticity and Plasticity*, Pergamon Press, Oxford (1975).
4. V. G. Karnaukhov and V. V. Mikhailenko, *Nonlinear Single-Frequency Vibrations and Dissipative Heating of Piezoelectric Inelastic Bodies* [in Russian], ZhGTU, Zhitomir (2005).
5. V. G. Karnaukhov, V. I. Kozlov, and T. V. Karaukhova, "The influence of shear strains on the efficiency of operation of piezoelectric sensors and actuators in active damping of the resonant vibrations of inelastic plates and shells," *Soprot. Mater. Teor. Sooruzh.*, **94**, 75–95 (2015).
6. V. D. Kubenko, P. S. Koval'chuk, and N. P. Podchasov, *Nonlinear Vibrations of Cylindrical Shells* [in Russian], Vyshcha Shkola, Kyiv (1989).
7. I. A. Motovilovetz and V. I. Kozlov, *Thermoelasticity*, Vol. 1 of the five-volume series *Mechanics of Coupled Fields in Structural Members* [in Russian], Naukova Dumka, Kyiv (1987).
8. V. G. Karnaukhov and I. F. Kirichok, *Electrothermoviscoelasticity*, Vol. 4 of the five-volume series *Mechanics of Coupled Fields in Structural Members* [in Russian], Naukova Dumka, Kyiv (1988).
9. F. Alijani and M Amabili, "Nonlinear vibrations of shells: A literature review from 2003 to 2013," *Int. J. Nonlin. Mech.*, **58**, No. 1, 233–257 (2014).
10. F. Allahkarami, M. G. Saryazdi, and M. Nikkhah-Bahrami, "Nonlinear forced vibration of a curved microbeam resting on nonlinear foundation using the modified strain gradient theory," *Int. Appl. Mech.*, **54**, No. 6, 718–738 (2018).
11. M. Amabili and M. P. Paidoussis, "Review of studies on geometrically nonlinear vibrations and dynamics of circular cylindrical shells and panels with and without fluid structure interaction," *Appl. Mech. Reviews*, **56**, No. 4, 349–381 (2003).
12. M. Amabili, *Nonlinear Mechanics of Shells and Plates in Composite*, *Soft and Biological Materials*, Cambridge University Press, Cambridge (2018).
13. A. Bhimaraddi, A. J. Carr, and P. J. Moss, "A shear deformable finite element for the analysis of general shells of revolution," *Computers & Struct.*, **31**, No. 3, 299–308 (1989).
14. J. Chroscielewski, R. Schmidt, and V. A. Eremeev, "Nonlinear finite element modeling of vibration control of plane rod-type structural members with integrated piezoelectric patches," *Continuum Mech. Thermodynam.*, **31**, No. 1, 147–188 (2019).
15. V. G. Karnaukhov, I. F. Kirichok, and V. I. Kozlov, "Thermomechanics of inelastic thin-walled structural members with piezoelectric sensors and actuators under harmonic loading (review)," *Int. Appl. Mech.*, **53**, No. 1, 6–58 (2017).
16. I. F. Kirichok and O. A. Cherniushok, "Axisymmetrical vibrations and vibroheating of thermoviscoelastic cylindrical shell with piezoactuators and shear deformation taken into account," *Int. Appl. Mech.*, **56**, No. 3, 340–346 (2020).
17. I. F. Kirichok and O. A. Cherniushok, "Forced vibrations and self-heating of a thermoviscoelastic cylindrical shear compliant shell with piezoelectric actuators and sensors" *Int. Appl. Mech.*, **56**, No. 6, 723–731 (2020).
18. V. I. Kozlov, "Oscillation and dissipative heating of a multilayer shell of revolution made of viscoelastic material," *Int. Appl. Mech.*, **32**, No. 6, 480–486 (1996).
19. V. I. Kozlov, T. V. Karnaukhova, and M. V. Peresun'ko, "Numerical modeling of the active damping of forced thermomechanical resonance vibrations of viscoelastic shells of revolution with the help of piezoelectric inclusions," *J. Math. Sci.*, **171**, No. 5, 565–578 (2010).
20. V. I. Kozlov, L. P. Zinchuk, T. V. Karnaukhova, and V. M. Sichko, "Forced geometrically nonlinear vibrations of thin shells of revolution with piezoelectric layers," *Int. Appl. Mech.*, **57**, No. 2, 200–216 (2021).
21. V. D. Kubenko and P. S. Koval'chuk, "Nonlinear problems of the vibration of thin shells (Review)," *Int. Appl. Mech.*, **34**, No. 8, 703–728 (1998).
22. V. D. Kubenko and P. S. Koval'chuk, "Stability and nonlinear vibrations of closed shells interacting with a fluid flow (review)," *Int. Appl. Mech.*, **51**, No. 1, 12–63 (2015).
23. C. J. Liu, Z. L. Zheng, X. Y. Yang, and J. J. Guo, "Geometric nonlinear vibration analysis for pretensioned rectangular orthotropic membrane," *Int. Appl. Mech.*, **54**, No. 1, 104–119 (2018).

24. J. M. S. Moita, C. M. M. Soares, and C. A. M. Soares, “Geometrically nonlinear analysis of composite structures with integrated piezoelectric sensors and actuators,” *Compos. Struct.*, **57**, No. 1, 1–4 (2002).
25. M. N. Rao, R. Schmidt, and K. U. Schroder, “Static and dynamic FE analtsis of piezolaminated composite shells considering electric field nonlinearity under thermo-electro-mechanical loads,” *Acta Mechanica*, **229**, No. 12, 5093–5120 (2018).
26. R. G. Sabat, B. Mukherjee, W. Ren, and G. Yung, “Temperature dependence of the complete material coefficients matrix of soft and hard doped piezoelectric lead zirconate titanate ceramics,” *J. Appl. Phys.*, **101**, No. 6, 1–7 (2007).
27. S. Zhang, G. Zhao, M. N. Rao, R. Schmidt, and Y. Yu, “A review on modeling techniques of piezoelectric integrated plates and shells,” *J. of Intelligent Mater. Syst. Struct.*, **30**, No. 8, 1133–1147 (2019).